Arab J Sci Eng (2018) 43:1761–1776
https://doi.org/10.1007/s13369-017-2732-7

RESEARCH ARTICLE - CIVIL ENGINEERING

The Effect of LRB Parameters on Structural Responses for Blast and Seismic Loads

Muhammed Zain Kangda[1] · **Sachin Bakre**[1]

Received: 31 January 2017 / Accepted: 13 July 2017 / Published online: 25 July 2017
© King Fahd University of Petroleum & Minerals 2017

Abstract In the present paper, passive control technique such as base isolation system is studied under earthquake ground motions and underground blast-induced vibrations. The performance of the lead rubber bearing (LRB), idealized as Bouc–Wen model in mitigating the structural responses of a five-storey building model, is investigated. The earthquake ground motions are selected from ground motion database available on the portal COSMOS Virtual Data Centre, whereas the underground blast is modeled as an exponential decaying function as prescribed by Carvalho and Battista (Proc Inst Civ Eng Struct Build 156(3):243–253, 2003). The aim of the study is to analyze the effect of isolation parameters such as damping ratio, yield strength, post-yield stiffness ratio and yield displacement on the structural responses of the base-isolated building. Newmark's step-by-step integration method is adopted to evaluate the structural responses of the building. It is observed that the LRB is very effective in reducing the structural accelerations and storey drifts induced in the building due to ground-induced vibration. The comparison of results show that high value of yield strength harvests low bearing displacement and low percentage reduction in the top floor absolute acceleration. In addition, the study also evaluates the energy dissipated by the isolated structure. The energy dissipated by the base-isolated (LRB) building subjected to blast-induced vibrations, show that an optimum value of yield strength is found to be in the range of 10–20% of the total weight of the structure.

Keywords Blast-induced vibration · Bouc–Wen model · Earthquake · Hysteretic energy · Isolation parameters

✉ Muhammed Zain Kangda
zainkangda@gmail.com

[1] Visvesvaraya National Institute of Technology, Nagpur, India

1 Introduction

The catastrophic destructions caused by the natural hazards such as earthquakes and man-made activities like mine blasting, accidental explosions and terrorism over the years have made the structural engineering community vigilant. The earthquake problem is rather old, and since the early 1900s, the structural researchers have succeeded in developing structural analysis and design techniques for earthquake-resistant structures. A lot of developments in the design codes of seismic loads in the past decade have enabled engineers to control the failure of structures when subjected to the above-mentioned natural hazard. However, the structural damages caused by blast-induced vibrations pose challenges for the present engineers. Unlike seismic and wind loads, blast loads are a short duration phenomenon. Though, a blast occurs for milliseconds, it is capable of causing hazardous damage to structures and human life. The threats from such extreme loading conditions urge efforts to develop methods of structural analysis and design to resist blast load. In India, the blast-resistant design of structures is categorized as explosion above ground IS 4991 [1] and underground blasts IS 6922 [2]. In addition, different international codes and regulations [3–5] provide guidelines to mitigate blast-induced effects on structures. In the present study, the structural responses are evaluated for underground blast-induced vibrations. Dowding [6] evaluated the vibration response of structures subjected to underground blasting. Wu et al. [7] conducted blasting experiments on rock surface to study and record ground accelerations. Later Wu and Hao [8] validated the recorded data with the help of a numerical model. The study was further extended to investigate the structural response subjected to underground blast-induced vibration. Carvalho and Battista [9] investigated the structural response of a RC framed structure subjected to blast-induced vibra-

tion theoretically and experimentally. The blast was modeled as an exponential decaying function to obtain blast-induced ground acceleration, $\ddot{x}_g\ (t)$ given by Eq. 1:

$$\ddot{x}_g(t) = -\frac{1}{t_d} v e^{\frac{-t}{t_d}} \tag{1}$$

The peak particle velocity (PPV) is represented by v (m/s), whereas t_d is the arrival time $= R/c$. R (m) is the distance between the charge centre and structure undergoing vibration due to the explosion, and c is wave propagation velocity (m/s) in soil obtained as the square root ratio of E and γ_d where E is Young's modulus in N/m^2 and γ_d is the average mass density in kg/m^3. Empirical formulae to predict the blast-induced vibrations in terms of PPV as proposed by various researchers, based on soil site condition, have been summarized and proposed by Kumar et al. [10]. Recently, Kumar et al. [11] proposed an empirical model to obtain PPV values considering various rock parameters. Hence, extensive studies to monitor the propagation of blast waves are being conducted. However, the techniques to protect and prevent existing and new structures from the damages caused by blast loads require considerable attention.

In recent years, various vibration control methods such as passive control systems, active control systems and hybrid systems have been developed either to minimize seismic forces acting on the structure or to absorb the forces which in turn reduce the damages incurred to the structure. It may be noted that these vibration control methods have been studied widely in the field of earthquake engineering, but its application to blast-induced vibration is limited [12–14]. Thus, the present study implements the concept of passive system, i.e., base isolation system to study the structural response under blast-induced vibrations. In the last few decades, a lot of technological evolution and development have happened in the field of earthquake protection. A wide range of experimental work has been done on the configurations and materials used in the base isolation technique [15–17]. Constantinou and Tadjbakhsh [18] used the Wen's model [19] to optimize the performance of base-isolated system subjected to ground acceleration. Kelly et al. [20] proposed the use of base isolation combined with active control to minimize the damage caused by earthquakes to the structures. Ramallo et al. [21] analyzed the peak responses of a two-degree-of-freedom (2DOF) and 6DOF system using low elastomeric bearings and MR dampers. Recently, Ghodke and Jangid [22] proposed a linear model of shape memory alloy to analyze base-isolated structures subjected to earthquake excitations. Jangid [23] investigated the response of a multi-storey isolated structure mounted on lead rubber bearings subjected to seismic excitations. The variations of responses under the system were computed for the variation of isolator parameters. In the present study, similar approach is employed to investigate the structural response of base-isolated structures subjected to blast- induced loading. The objectives of the study also include evaluation of vibration energy dissipated by the selected base-isolated building model. The results obtained from the present study are also compared with the seismic response of the selected model. The base isolation device is modeled as prescribed by Constantinou and Tadjbakhsh and Wen.

2 Mathematical Model of Base-Isolated System

In the present study, Bouc–Wen model (BWM) is selected to model the nonlinear behavior of a base isolation system such as lead rubber bearings, LRB popularly known as N–Z bearing system. In the field of structural vibration control, the versatility of BWM to match the experimental hysteretic behavior of various types of damping devices along with base isolation systems [18] has made it popular. Moreover, the model is represented mathematically as the first-order nonlinear differential equation that relates input displacement to output restoring force in a hysteretic way [24]. Figure 1 shows the schematic representation of BWM studied by Marano and Greco [25] as a single-degree-of-freedom (SDOF) non-

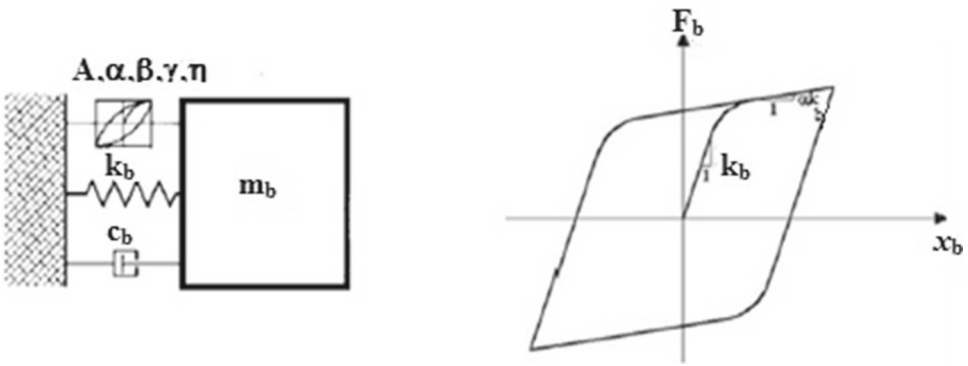

Fig. 1 Schematic representation of a Bouc–Wen model with its hysteretic behavior [25]

linear system having mass m_b, stiffness k_b and damping c_b along with its dimensionless shape parameters. The hysteretic restoring force, F_b, developed in the isolation device is expressed by Eq. 2.

$$F_b = \alpha \frac{F_y}{q} x_b + (1-\alpha)\, F_y Z \tag{2}$$

In Eq. 2, Z is a dimensionless hysteretic component satisfying the following nonlinear first-order differential equation given by Eq. 3:

$$q\dot{Z} = -\gamma|\dot{x}_b|Z|Z|^{\eta-1} - \beta\dot{x}_b|Z|^{\eta} + A\dot{x}_b \tag{3}$$

In the above expressions, q is the yield displacement given by F_y/k_b and F_y is the yield force and x_b, $\dot{x}_b$ and $\ddot{x}_b$ are the displacement, velocity and acceleration of the isolating device, respectively. β, γ and A are the dimensionless shape parameters. Parameter η is an integer which controls the smoothness of the transition from elastic to plastic response, and α is the post- to pre-yielding stiffness ratio. In the present study, the values of the above-mentioned dimensionless parameters are $A = 1$, $\beta = 0.5$, $\gamma = 0.5$ and $\eta = 1$. These parameters only affect the shape of hysteretic loop and have no influence on the performance of the dissipating device. The importance of post-yield stiffness ratio, α, to obtain the isolation period, T_b, of the LRB system is also incorporated in the study. Equation 4 calculates the time period of the base isolation, where $M = (m_b + m_s)$ is the total mass of the building such that m_b is the mass of isolating device and m_s is the total structural mass of the building at different storey levels. The viscous damping, c_b, developed in the isolating device is obtained from the damping ratio, ξ_b given by Eq. 5 from base isolation frequency $\omega_b = 2\pi/T_b$. Thus to model a LRB system using BWM, four primary parameters are required, namely the isolation period (T_b), damping ratio (ξ_b), yield displacement (q) and normalized yield strength (F_0) obtained as a ratio of yield strength of the bearing (F_y) and total weight of the isolated building, $W = Mg$ given by Eq. 6, g is the acceleration due to gravity.

$$T_b = 2\pi\sqrt{\frac{M}{\alpha k_b}} \tag{4}$$

$$c_b = 2\xi_b M\omega_b \tag{5}$$

$$F_0 = \frac{F_y}{W} \tag{6}$$

The isolating mechanism supports an idealized multi-storey building as shown in Fig. 2. The study analyzes the performance of the building with and without base isolation system subjected to blast and seismic excitations. The generalized equation of motion of a multi-storey building in matrix form subjected to seismic excitation $\ddot{x}_g$ is given by Eq. 7. The mass matrix of the building M_s is a diagonal matrix, whereas C_s and K_s are the damping and stiffness matrix of the structure which are symmetrical and of the order $n \times n$ where n is the total number of floors of the superstructure. The vector {1} is a unity vector of the order nx1 having for all its elements unity, and $\{x\}$ and $\{\dot{x}\}$ are the displacement and velocity vectors of the superstructure. The acceleration of base mass relative to ground is denoted by $\ddot{x}_b$.

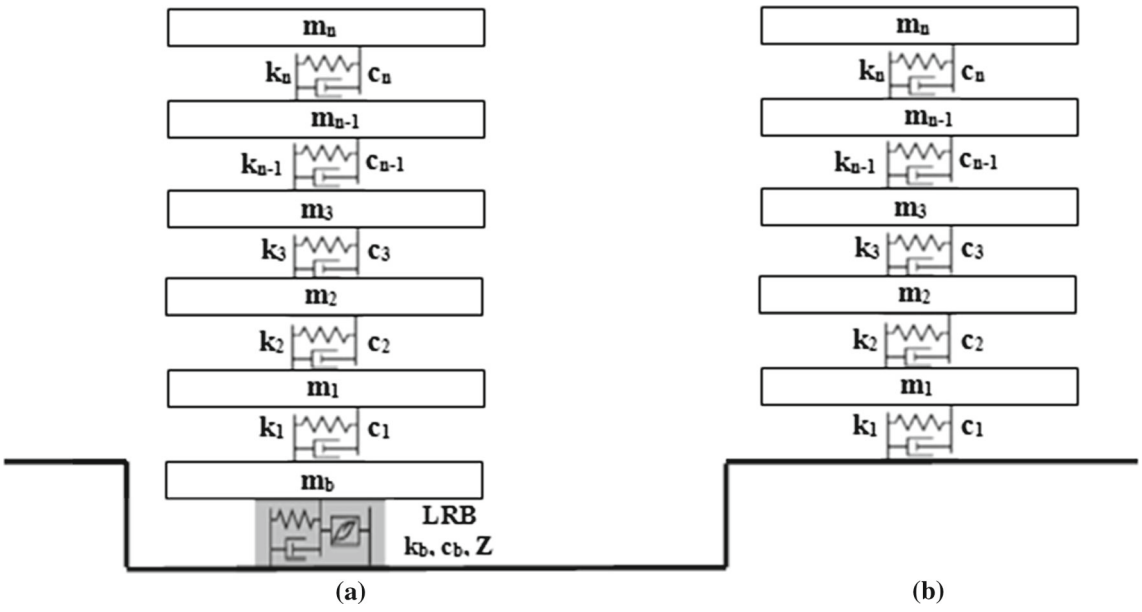

Fig. 2 Idealized model of multi-storey building, **a** with and **b** without isolation system [28]

Table 1 Peak ground acceleration of the selected ground motion

Sr. no.	Earthquake motions	Station name	PGA (m/s^2)	PGV (m/s)
1	Imperial Valley Earthquake, 1979	El Centro Array #5	3.6	0.96
2	Loma Prieta Earthquake, 1989	Corralitos—Eureka Canyon	4.69	−0.47
3	Northridge Earthquake, 1994	Sylmar—County Hospital	5.92	−0.77

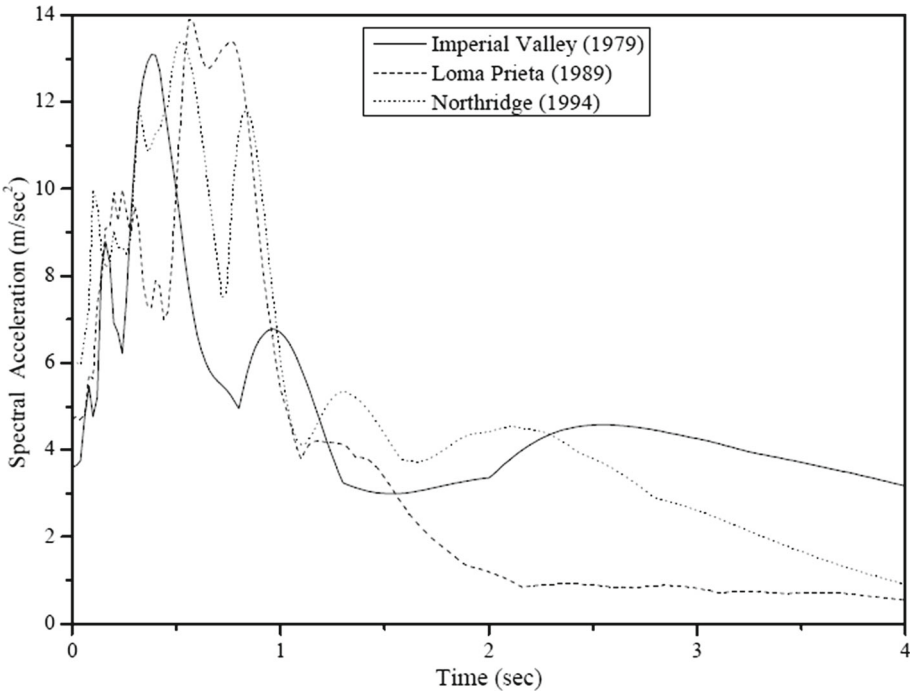

Fig. 3 Response spectra for selected ground motions (5% damping)

$$[M_s]\{\ddot{x}\} + [C_s]\{\dot{x}\} + [K_s]\{x\} = -[M_s]\{1\}\left\{\ddot{x}_g + \ddot{x}_b\right\} \tag{7}$$

Moreover, the governing equation of motion of the isolating device as expressed by Jangid [23] having mass m_b subjected to seismic excitation, $\ddot{x}_g$, is given by Eq. 8.

$$m_b\ddot{x}_b + c_b\dot{x}_b + F_b - c_1\dot{x}_1 - k_1x_1 = -m_b\ddot{x}_g \tag{8}$$

In the above equation, c_1 and k_1 are the first floor damping and stiffness of the superstructure as shown in Fig. 2. Due to nonlinear force–deformation behavior of the isolated structure, the governing equation cannot be solved using the classical modal superposition technique, Jangid [23]. As a result, the Newmark's step-by-step integration method is adopted assuming linear variation of acceleration to study the structural response over the time interval, dt. The maximum time interval dt for earthquake motions as tabulated in Table 1 is 0.005 s and for blast loading as discussed in Sect. 3, dt = 0.0005 s. Figure 3 shows the spectral acceleration curves obtained from the selected times histories to represent the properties of ground motion. The criteria for selection of accelerogram data are based on the Eurocode 8 Part 1 and compiled by Iervolino et al. [29] as follows:

(a) A minimum of 3 accelerogram should be used;
(b) the mean of the zero period spectral response acceleration values (calculated from the individual time histories) should not be smaller than the value of ag S for the site in question;
(c) in the range of periods between 0.2T1 and 2T1, where T1 is the fundamental period of the structure in the direction where the accelerogram will be applied, no value of the mean 5% damping elastic spectrum, calculated from all time histories, should be less than 90% of the corresponding value of the 5% damping elastic response spectrum.

The energy equations derived by Uang and Bertero [26] are also incorporated in the study to estimate the vibration energy capacity of the nonlinear model under the effect of blast and seismic ground shaking. The total input energy (E_i) is defined as the work done on the structure by the applied inertia force and is determined by Eq. 9. The input energy is also expressed as the sum of kinetic energy, damping energy, elastic strain energy and hysteretic energy given by Eq. 10.

$$E_i = \int_0^t M_s\ddot{x}_g \mathrm{d}\dot{x}\ \mathrm{d}t \tag{9}$$

$$E_{\mathrm{i}} = E_{\mathrm{k}} + E_{\xi} + E_{\mathrm{s}} + E_{\mathrm{h}} = E_{\mathrm{k}} + E_{\xi} + E_{\mathrm{a}} \tag{10}$$

The kinetic energy (E_{k}) is expressed as the sum of the masses (M), and their corresponding velocities ($\dot{x}$) for the structure are obtained by Eq. 11 and the nonnegative damping energy (E_{ξ}) of the system is calculated by Eq. 12. The energy absorbed by the system (E_{a}) is composed of recoverable elastic strain energy (E_{s}) and irrecoverable hysteretic energy (E_{h}) and determined by Eqs. 13, 14 and 15, respectively.

$$E_{\mathrm{k}} = \frac{M_s \dot{x}^2}{2} \tag{11}$$

$$E_{\xi} = \int_0^t C_S \dot{x} \mathrm{d}x = \int_0^t C_S \dot{x}^2 \mathrm{d}t \tag{12}$$

$$E_{\mathrm{a}} = \int_0^t F_b \dot{x} \mathrm{d}t = E_{\mathrm{s}} + E_{\mathrm{h}} \tag{13}$$

$$E_{\mathrm{s}} = \frac{(F_b)^2}{2k_b} \tag{14}$$

$$E_{\mathrm{h}} = E_{\mathrm{a}} - E_{\mathrm{s}} \tag{15}$$

3 Model to Predict Blast-Induced Ground Acceleration

As discussed in Introduction, various researchers have proposed different empirical formulae to predict the peak particle velocity based on the site conditions. Extensive field blast tests have been carried out to assess the PPV for dif-

Table 3 Structural parameters of a five-storey model, $T_b = 2.5$ s and $\xi_b = 4\%$

Floor masses (kg)	Stiffness coefficients (kN/m)	Damping coefficients (kN s/m)
$m_b = 61200$	$\alpha k_b = 2129.8$	$c_b = 69.938$
$m_1 = 53073$	$k_1 = 101196$	$c_1 = 348.140$
$m_2 = 53073$	$k_2 = 87279$	$c_2 = 301.380$
$m_3 = 53073$	$k_3 = 85863$	$c_3 = 296.18$
$m_4 = 53073$	$k_4 = 74862$	$c_4 = 259.81$
$m_5 = 53073$	$k_5 = 57177$	$c_5 = 197.45$

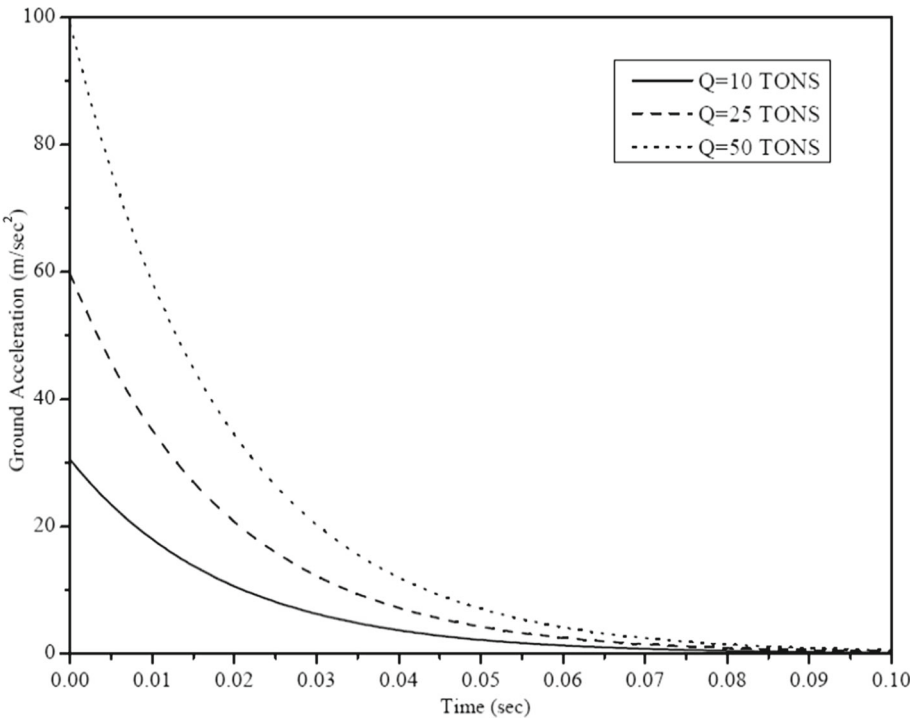

Fig. 4 Blast-induced ground acceleration time histories

Table 2 Summary of peak particle velocities

Sr. no.	Charge mass, Q (tons)	Charge centre distance, R (m)	Peak particle velocity, v (m/s)	Scaled distance, SD (m/kg$^{1/2}$)	Wave propagation velocity, $c = \sqrt{(E/\gamma_{\mathrm{d}})}$ (m/s)	Arrival time, t_{d} (s)
1	10	100	0.58	1.0	5280	0.0189
2	25	100	1.13	0.63	5280	0.0189
3	50	100	1.87	0.45	5280	0.0189

Table 4 Structural responses of a fixed-base building model

Base excitation	Base displacement (mm)	Top storey absolute acceleration (g)	Top storey drift (mm)	Top storey displacement (mm)
$Q = 10$ tons	14.03	1.54	13.9	66.34
$Q = 25$ tons	27.42	3.0	27.26	129.67
$Q = 50$ tons	45.53	5.0	45.26	215.3
Imperial valley	22.43	1.24	11.24	91.78
Loma prieta	36.72	2.34	21.3	160.0
Northridge	38.92	2.94	23.94	177.65

Table 5 Performance of five-storey building mounted on the selected isolators having $\alpha = 0.05$

Excitation	Yield strength ratio (F_0)	LRB1			LRB2		
		Bearing displacement (mm)	Top storey acceleration (% reduction)	Top storey drift (% reduction)	Bearing displacement (mm)	Top storey acceleration (% reduction)	Top storey drift (% reduction)
Blast = 10 tons	0.025	176	86.69	86.55	162	83.83	83.67
	0.10	116	71.56	71.44	110	68.90	68.78
	0.15	96	63.51	63.31	91	61.04	61.15
	0.2	80	57.21	56.98	76	55.65	55.40
	0.3	59	48.57	48.20	57	47.79	47.48
Blast = 25 tons	0.025	374	87.87	87.82	344	86.40	86.43
	0.10	290	81.27	81.29	269	78.10	78.14
	0.15	252	76.00	75.94	237	73.00	73.04
	0.2	225	71.00	71.09	213	68.43	68.45
	0.3	185	63.00	62.91	176	61.00	60.90
Blast = 50 tons	0.025	642	88.34	88.27	590	87.48	87.45
	0.10	550	85.88	85.86	508	82.52	82.48
	0.15	498	82.42	82.39	460	79.20	79.16
	0.2	452	79.20	79.05	421	76.00	75.98
	0.3	390	73.00	72.89	368	70.20	70.17
Imperial Valley (1979)	0.025	550	73.71	66.90	453	74.52	72.15
	0.10	230	69.03	68.95	213	68.79	68.68
	0.15	180	67.90	67.79	166	67.58	67.44
	0.2	140	67.18	60.85	131	66.85	63.35
	0.3	97	66.13	56.67	92	65.89	58.99
Loma Prieta (1989)	0.025	100	90.38	90.44	94	90.00	89.96
	0.10	86	74.79	74.74	84	75.35	75.30
	0.15	80	68.68	68.83	79	69.53	69.49
	0.2	74	64.10	64.18	71	64.93	64.87
	0.3	72	57.26	57.56	70	58.94	58.85
Northridge (1994)	0.025	435	87.04	85.38	329	88.61	87.26
	0.10	220	84.05	82.21	189	83.30	81.41
	0.15	164	77.35	74.81	150	76.90	74.23
	0.2	143	72.79	69.67	136	72.65	69.51
	0.3	137	67.93	64.24	132	68.03	64.41

Table 6 Performance of five-storey building mounted on the selected isolators having $\alpha = 0.3$

Excitation	Yield strength ratio (F_0)	LRB1			LRB2		
		Bearing displacement (mm)	Top storey acceleration (% reduction)	Top storey drift (% reduction)	Bearing displacement (mm)	Top storey acceleration (% reduction)	Top storey drift (% reduction)
Blast = 10 tons	0.025	186	87.14	87.05	171	85.45	85.32
	0.10	148	83.25	83.17	139	81.23	81.15
	0.15	139	81.88	81.80	131	80.19	80.07
	0.2	133	81.10	81.01	126	79.61	79.50
	0.3	127	80.19	80.00	121	78.90	78.78
Blast = 25 tons	0.025	384	88.00	88.00	353	86.97	86.98
	0.10	328	85.67	85.66	303	83.17	83.20
	0.15	304	84.20	84.19	283	81.90	81.91
	0.2	289	83.10	83.13	270	81.10	81.11
	0.3	270	81.67	81.77	254	80.07	80.08
Blast = 50 tons	0.025	653	88.40	88.33	600	87.80	87.76
	0.10	590	86.80	86.74	543	84.84	84.80
	0.15	555	85.94	85.88	512	83.56	83.52
	0.2	527	85.08	85.02	488	82.66	82.59
	0.3	490	83.54	83.47	456	81.44	81.37
Imperial Valley (1979)	0.025	597	71.85	64.86	490	73.47	69.31
	0.10	298	75.40	75.27	251	76.45	76.33
	0.15	220	75.32	75.18	210	76.21	76.16
	0.2	200	74.68	74.56	191	75.65	75.53
	0.3	177	73.71	73.58	173	74.52	74.47
Loma Prieta (1989)	0.025	100	93.89	93.87	89	93.38	93.38
	0.10	126	91.97	90.86	123	91.41	91.41
	0.15	150	90.68	89.39	139	90.17	90.14
	0.2	160	89.79	88.17	147	89.40	89.44
	0.3	174	87.52	86.43	156	88.29	88.03
Northridge (1994)	0.025	490	86.26	84.54	375	88.67	87.34
	0.10	306	88.20	86.80	264	89.35	88.10
	0.15	251	88.88	87.55	235	89.12	87.84
	0.2	233	88.20	86.63	226	88.57	87.26
	0.3	228	87.41	85.80	219	87.96	86.55

ferent types of soils and rock types. The PPV is the most important parameter to model blast- induced ground acceleration analytically. It is defined as the maximum velocity of ground particle in the given direction due to vibration caused by an explosion Mohamed and Mohamed [27]. The most generalized expression to predict PPV for any soil condition is as follows:

$$v = k\mathrm{SD}^{-b} \tag{16}$$

where v is the peak particle in m/s, SD is the scaled distance ($\mathrm{m/kg^{1/2}}$) determined as the ratio of distance from charge point, R (m), to the square root of charge mass, Q (kg), and k and b are site constants determined by blast experiments. In the present study, empirical equation proposed by Kumar et al. [11] is used to predict PPV as site constants require blast experiments. The PPV model considered various rock site parameters affecting blast wave propagation. The proposed empirical formula for calculation of PPV is established based on the curve fitting technique applied to the collected field blast data. The blast vibration values predicted from the proposed equation compare well with the field data cases. In the present study, the PPV is evaluated for a granite site having material constants specified by Wu and Hao [8]. The material constants for granite include Young's modulus, $E = 73.9$ GPa, average mass density, $\gamma_\mathrm{d} = 26.50\,\mathrm{kN/m^3}$, and uniaxial compressive strength, $f_\mathrm{c} = 70$ MPa. These constants are substituted in Eq. 17 to evaluate the PPV, for a constant value of charge centre, i.e., $R = 100$ m, and the charge mass is varied to plot the ground acceleration produced due to an underground blasting as shown in Fig. 4.

$$v = \frac{f_c^{0.642}\mathrm{SD}^{-1.463}}{\gamma_D} \tag{17}$$

A summary of peak particle velocities obtained from blast and rock properties to plot ground vibration is tabulated in

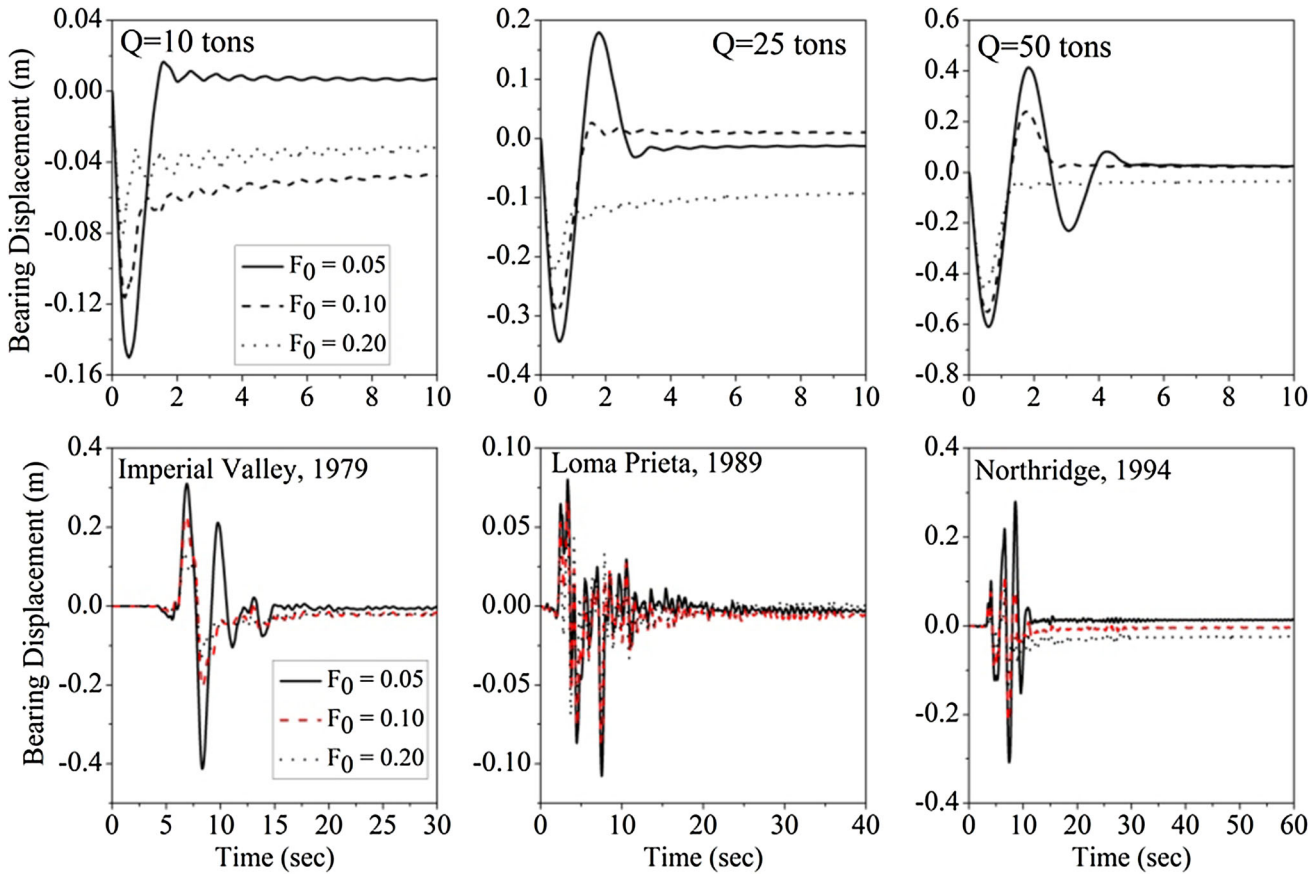

Fig. 5 Time variation of bearing displacement under selected ground excitations for $F_0 = 0.05$, 0.1 and 0.2

Table 2. The blast is modeled using the exponential decay function discussed by Carvalho and Battista.

4 Numerical Study

For the present study, a five-storey base-isolated structure investigated by Zhang and Philips [28] subjected to air blast loading is selected to investigate its performance under both underground blast and seismic loads. Zhang and Philips scaled the linear lumped parameter model (one third scale) investigated by Kelly et al. [20] to represent the full-scale superstructure as shown in Fig. 2. According to Zhang and Philips, for the fixed-base condition, the fundamental time period of the superstructure is $T_s = 0.54$ s and the structural damping ratio $\xi_s = 2\%$ in the first mode. For the base-isolated structure, $T_b = 2.5$ s and $\xi_b = 4$ and 10%. The structural properties of a five-storey base-isolated structure are tabulated in Table 3, and its responses are evaluated subjected to seismic and blast- induced vibration. The full-scale model with fixed-base condition is analyzed first under the effect of blast and earthquake excitation, and its responses are tabulated in Table 4. The peak top floor absolute acceleration is obtained as the sum of ground acceleration, and top floor acceleration and is expressed in terms of acceleration due to gravity (g). The performance of the five-storey superstructure is evaluated with the prescribed isolation technique.

As discussed in Sect. 2, the base-isolated structure is characterized by four parameters, i.e., the isolation period, damping ratio, yield displacement and normalized yield strength. For the present study, the time period of isolation is kept constant, whereas the study evaluates the performance of a base-isolated structure for two cases of damping ratios, i.e., $\xi_b = 4$ and 10%. The effect of post-yield stiffness ratio, normalized yield strength and yield displacement

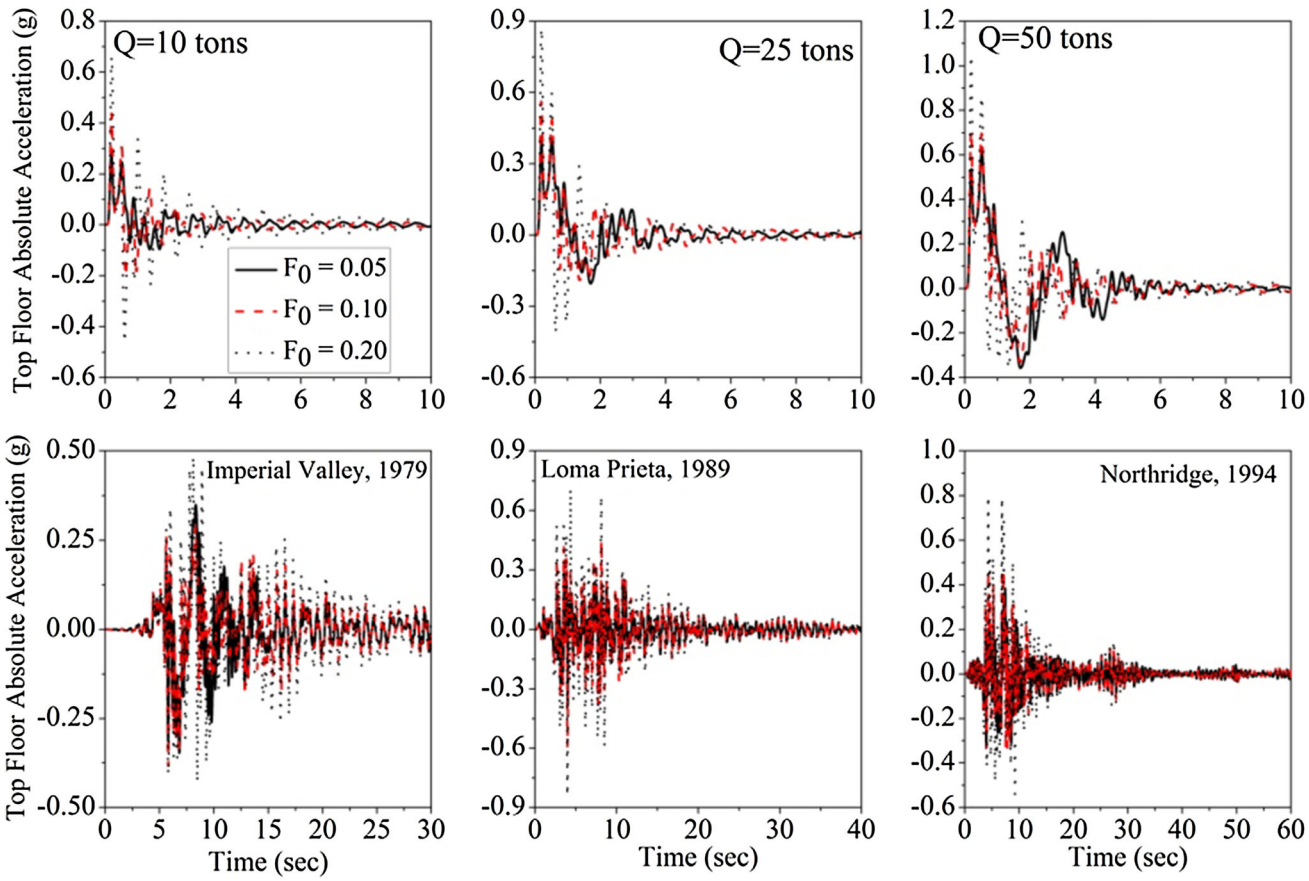

Fig. 6 Time variation of top floor absolute acceleration under selected ground excitations for $F_0 = 0.05$, 0.1 and 0.2

on the structural responses of the base-isolated building is also studied. The study is divided into three parts: in the first part, effect of post-yield stiffness ratio and normalized yield strength is discussed, and in the second part, effect of yield displacement and normalized yield strength is taken into account. Finally, the effect of damping ratio on the performance of the structure is tabulated in the Tables 5 and 6. The study incorporates the performance of two isolators, i.e., low damping isolators, LRB1 ($\xi_b = 4\%$) and high damping isolator, LRB2 ($\xi_b = 10\%$). The investigation of isolators based on the damping ratios, suggests that LRB1 is effective in mitigating the structural responses subjected to blast-induced vibrations as compared to LRB2. It is important to note that the bearing displacement values obtained from the blast analysis is almost 6% more in case of LRB1 to achieve the reduction in structural responses. The performance of LRB1 further improves with a higher post-yield stiffness ratio. However, the results obtained from the seismic analysis show that the LRB2 is more effective than LRB1 in reducing the structural responses. It is interesting to note that the performance of LRB1 as in case of Imperial Valley Earthquake at a low post-yield stiffness ratio of 0.05 shows better percentage reduction in storey drift and acceleration values. Thus, the performance of the lead rubber isolators depends on the ground motions under consideration and observation hold true as in case of the literature [21]. The time variation plots of bearing displacement, top floor absolute acceleration and hysteretic energy dissipated by the isolation system are also presented in the study. Figs. 5, 6 and 7 show the above-mentioned output results, respectively, under the selected earthquakes and blast- induced vibrations for a constant post-yield stiffness ratio, i.e., $\alpha = 0.05$ and $\xi_b = 4\%$. From Fig. 5, it can be observed that an increase in normalized yield strength (F_0) reduces the peak bearing displacement under the effect of blast loads and selected earthquake ground motions for the specified case, i.e., $\alpha = 0.05$. However, it

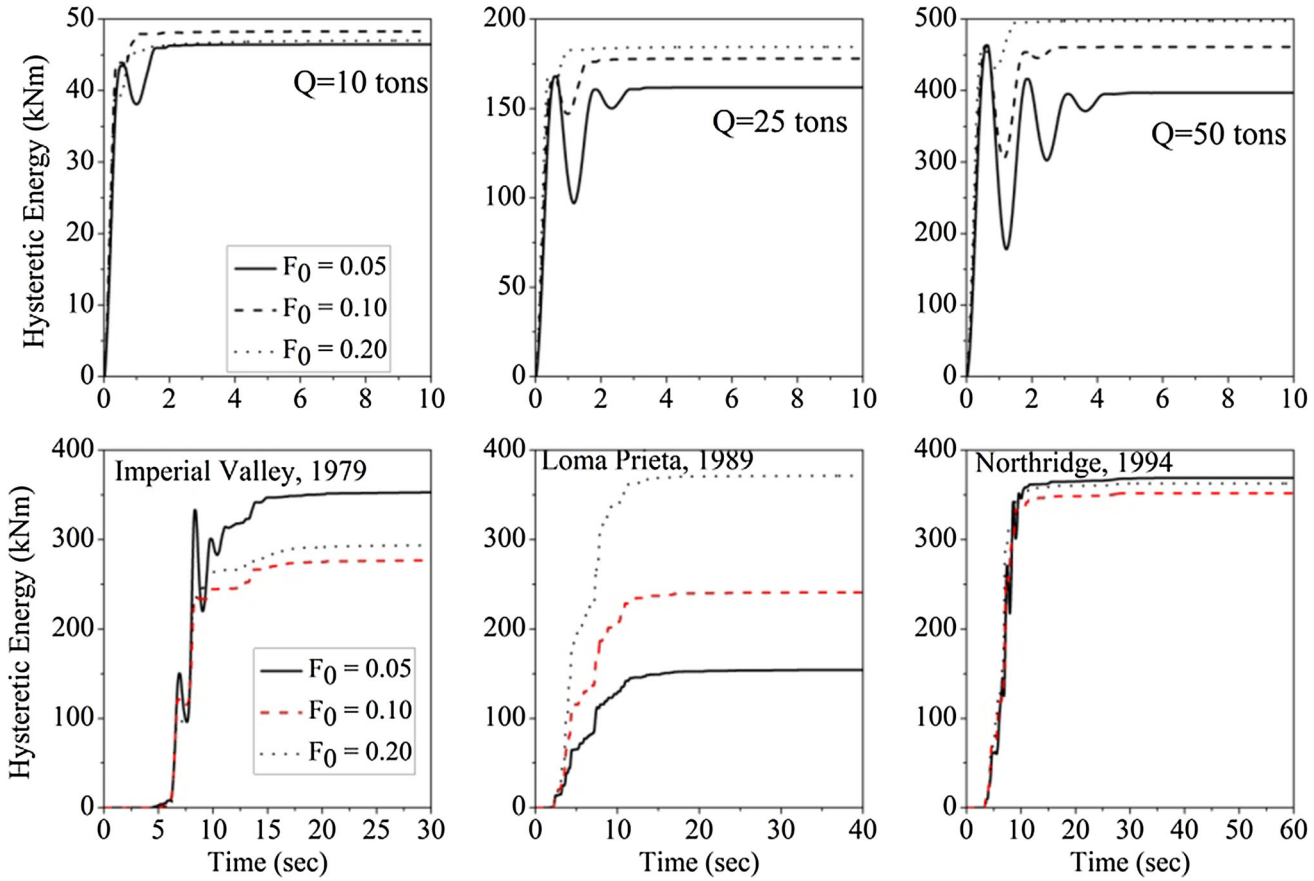

Fig. 7 Time variation of hysteretic energy dissipated under selected ground excitations for $F_0 = 0.05$, 0.1 and 0.2

can be observed in Fig. 8 that F_0 reduces the peak bearing displacement for all blast load cases and Imperial Valley and Northridge Earthquake. Moreover, a higher value of α leads to higher bearing displacement and the observation is satisfied by all blast and mentioned earthquakes. The Loma Prieta Earthquake shows an increase in bearing displacement for an increase in value of α, but for an increase in value of F_0, the behavior of the base-isolated structure is inconsistent due to the frequency content of the earthquake. Thus, a higher value of F_0 and lower value of α is favorable for a reduced peak bearing displacement. On the other hand, Fig. 6 advocates a selection of lower value of F_0 to obtain reduced peak top storey absolute acceleration for all selected ground motions.

From Fig. 9, it can be concluded that lower value of F_0 and higher α leads to higher percentage reduction in peak absolute acceleration values, i.e., lower value of absolute acceleration values. In case of the Imperial Valley, an increase in value of α shows a nonlinear behavior, but the values of peak absolute acceleration reduce for a lower value of F_0. The hysteretic energy dissipated by the isolating device is plotted against time for the selected case in Fig. 7. It is interesting to note that the isolating device dissipates maximum energy under blast with charge weight of 50 tons, whereas performance under the effect of earthquake is nearly same with Loma Prieta earthquake showing abrupt results. A plot of maximum hysteretic energy under the ground-induced vibration for two selected isolators, i.e., LRB1 and LRB2, is shown in Figs. 10 and 11, respectively. It is observed in the present study that a higher value of α results in low hysteretic energy for both the selected isolators. Moreover, an increase in the damping ratio further results in the reduction

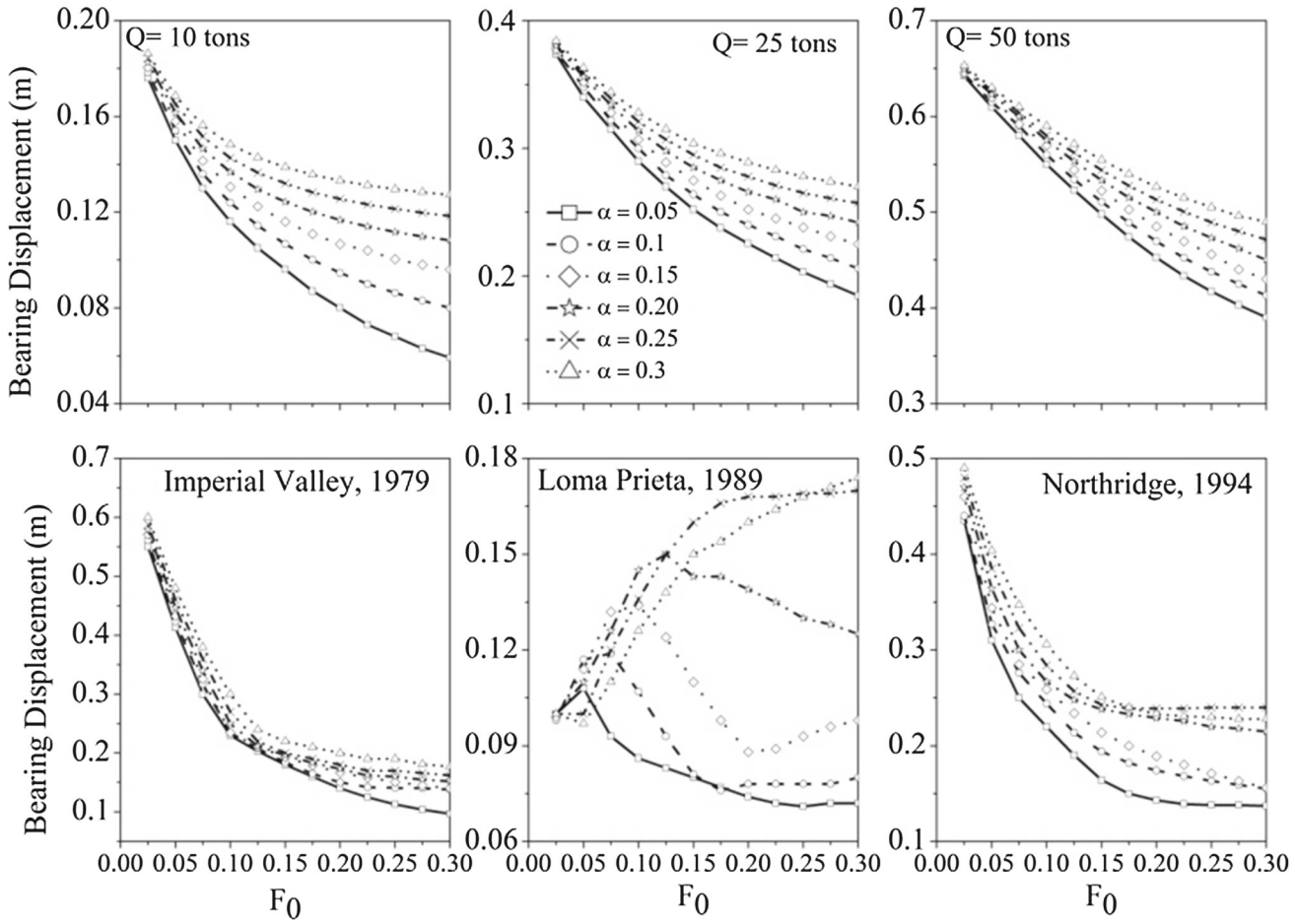

Fig. 8 Variation of peak bearing displacement against normalized yield strength F_0 for different values of α ($\xi_b = 4\%$)

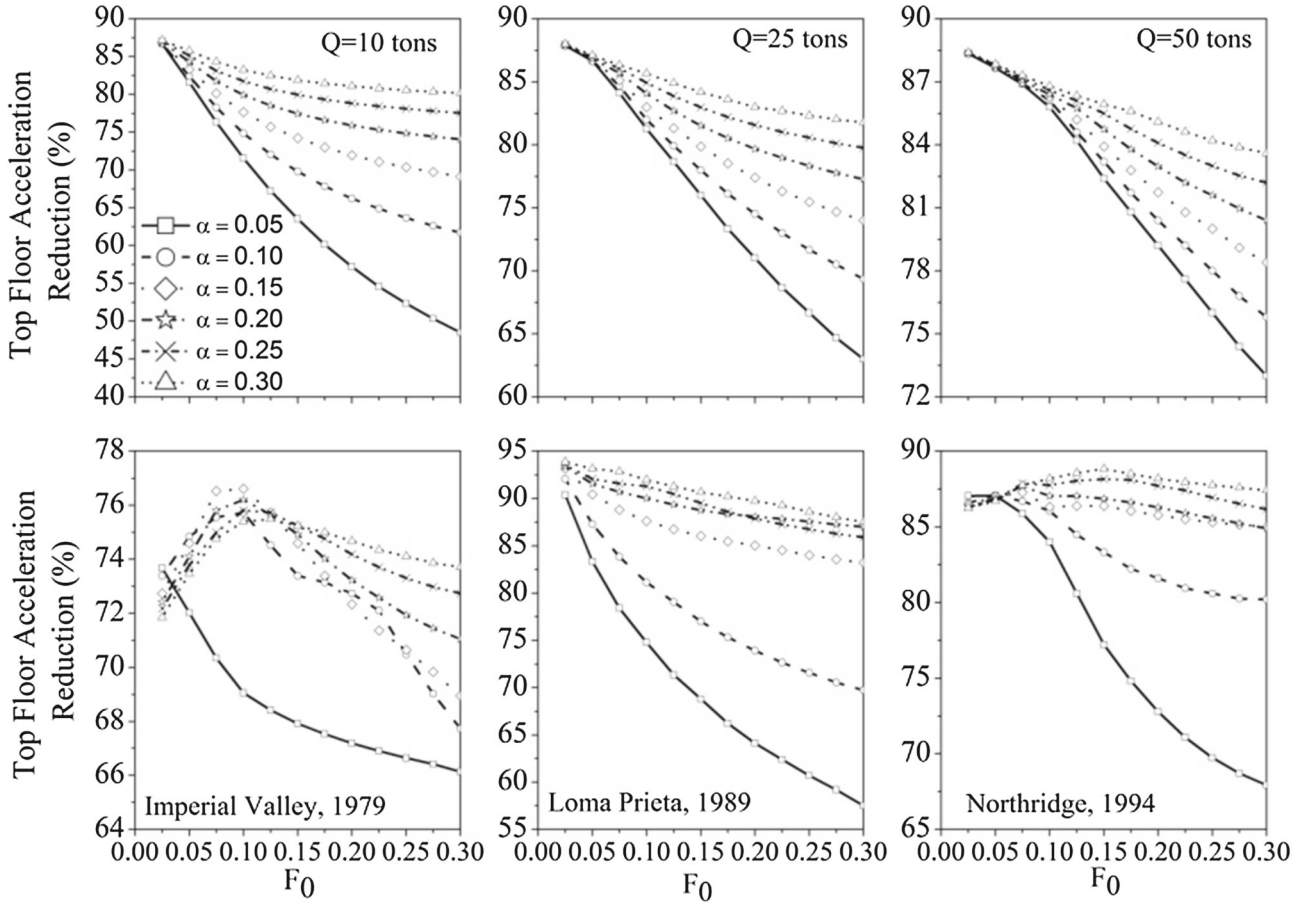

Fig. 9 Variation of peak top floor acceleration reduction against normalized yield strength for different values of α ($\xi_b = 4\%$)

of hysteretic energy as the bearing displacement reduces due to increase in damping in the isolator. It is also observed that in a lead rubber isolated building subjected to blast-induced vibrations, the optimum value of yield strength is found to be 10-20% of the total weight of the structure. The hysteretic energy dissipated as in case of seismic excitations shows a complicated nature; however, the optimum value of yield strength remains in the range specified for blast loading.

The effect of yield displacement (q) on the structural responses is also discussed in the present study. The yield displacement is restricted to 25 and 12.5 mm based on the restriction on the value of α not greater than 1. The value of F_0 is varied from 0.025 to 0.3, and the structural responses are plotted for LRB1 as shown in Fig. 12. It can be observed that for a restricted value of yield displacement the bearing displacement values decrease with increase in F_0 with a blast of 50 ton causing the most damaging effect on the isolating device.

The maximum bearing displacement for a 50 ton blast is as high as 0.67 m almost matching with the displacement caused by the Imperial Valley earthquake equal to 0.665 m. The percentage reduction in acceleration also decreases with an increase in normalized yield strength values. The performance of the LRB1 system in reducing the absolute acceleration under Loma Prieta earthquake is the most efficient, whereas for a higher F_0 the efficiency reduces and the 10 ton blast shows least reduction. The hysteretic energy

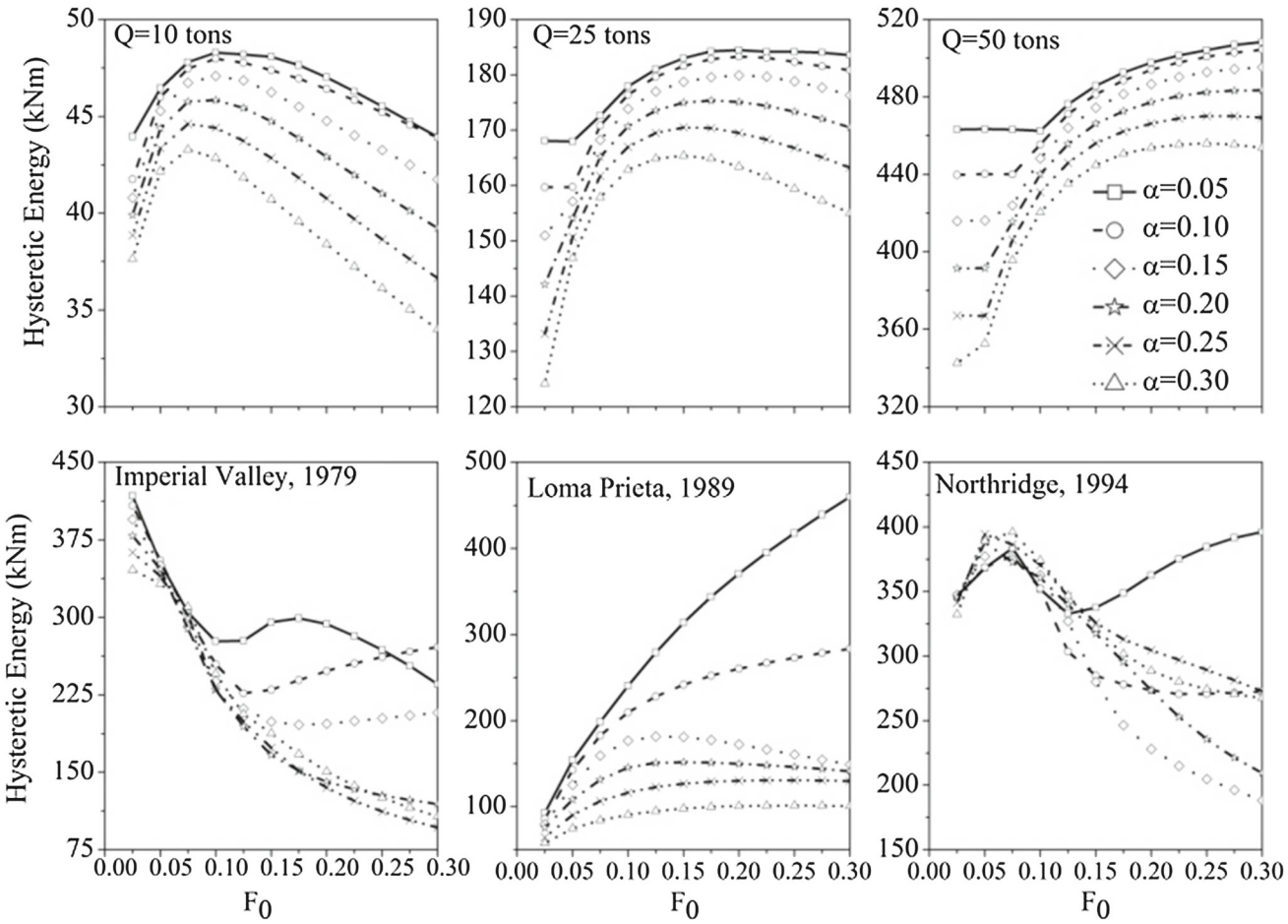

Fig. 10 Variation of hysteretic energy against normalized yield strength for different values of α ($\xi_b = 4\%$)

increases with increase in the value of F_0, and the blast of 50 ton causes the most damaging effect on the device. The Loma Prieta earthquake shows a linear increase the value of dissipated energy with yield strength, whereas the energy under the blast- induced vibration becomes almost constant for F_0 greater than 0.2. The comparison between two yield displacement values concludes that a lower yield displacement results in lower bearing displacement, but a higher yield displacement value (q) is beneficial to obtain least absolute acceleration value, i.e., higher percentage reduction in absolute acceleration. Moreover, higher value of q also reduces the hysteretic energy dissipated by the isolating device. The effect of yield displacement on the structure responses of a base-isolated building concludes that an optimum value of yield strength is found tp be in the range of 10–20% of the weight of the structure for different cases of earthquake loadings and blast- induced vibrations

5 Discussion and Conclusion

In the present study, base isolation technique is employed to a five- storey building subjected to underground blast and seismic excitations. The LRB plays a pivotal role in reducing the floor acceleration response and storey drift in the building. The peak bearing displacement, an important output result in the design of base isolation system, is also optimized using isolation parameters and plotted as shown in Fig. 8. The optimized isolation parameters are reported, and the effects on the structural responses are also plotted. An attempt is made to establish relation between energy dissipated with structural responses. The complex energy dissipating behavior of the isolated structure under the selected earthquakes is also discussed. The study outlines following conclusions from the detailed analysis of the isolated technique:

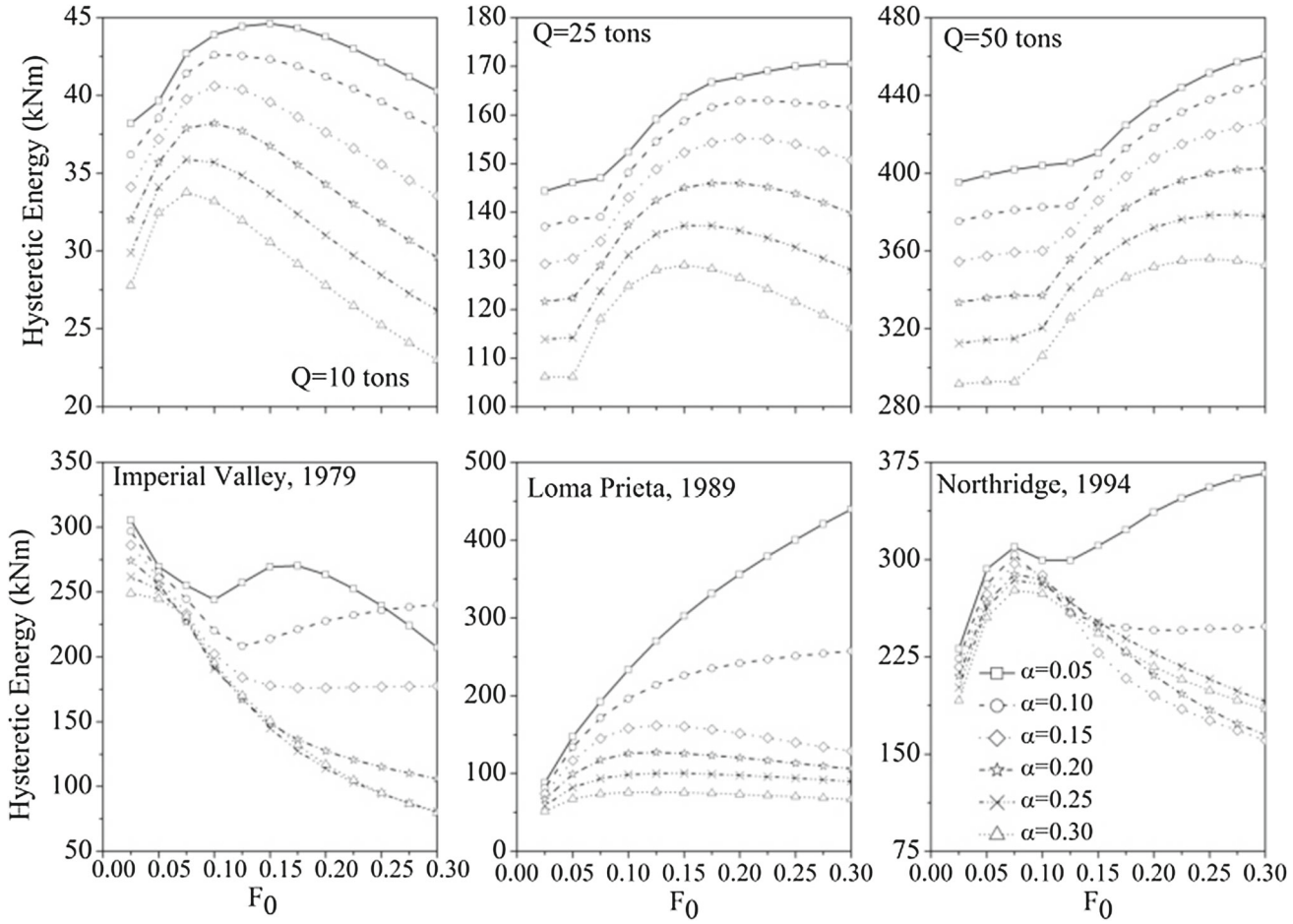

Fig. 11 Variation of hysteretic energy against normalized yield strength for different values of α ($\xi_b = 10\%$)

1. For a high value of normalized yield strength and constant post-yield stiffness ratio, a significant reduction in peak bearing displacement is obtained. Consequently, a combination of a low value of α and high value of F_0 yields least peak bearing displacement for all selected blast-induced vibrations.
2. The relationship between F_0 and top floor absolute acceleration values reports that high value of F_0 results in low percentage reduction in absolute acceleration response of the structure, i.e., high value of absolute acceleration. Thus, a higher percentage reduction in absolute acceleration values is achieved under the synthesis of low value of F_0 and high value of stiffness ratio.
3. The energy dissipated by the base-isolated structure reveal that an optimum value of normalized yield strength (F_0) is obtained in the range of 10–20% of the total weight of the structure subjected to blast-induced vibrations. However, the responses obtained under the effect of earthquake loading show complex behavior and depend on the frequency content of the excitation.
4. The structural responses obtained from the study based on the yield displacement parameter of base-isolated structure show that an optimum value of normalized yield strength (F_0) is obtained in the range of 10–20% of the weight of the structure.
5. The comparisons of the two selected isolators show that high damping isolator (LRB2) results in low hysteretic energy and bearing displacement.
6. The effect of damping ratio, ξ_b, in mitigating the structural responses such as storey drift and acceleration reduction is also investigated. The study compares the effectiveness of low damping isolator and high damping isolator in improving the structural performance under the two selected load cases, i.e., blast and earthquakes. The present study observed that low damping isolator is found to be more effective than high damping isolator under the blast load case, whereas high damping isolator shows better response reduction ability as compared to low damping isolator for seismic case.

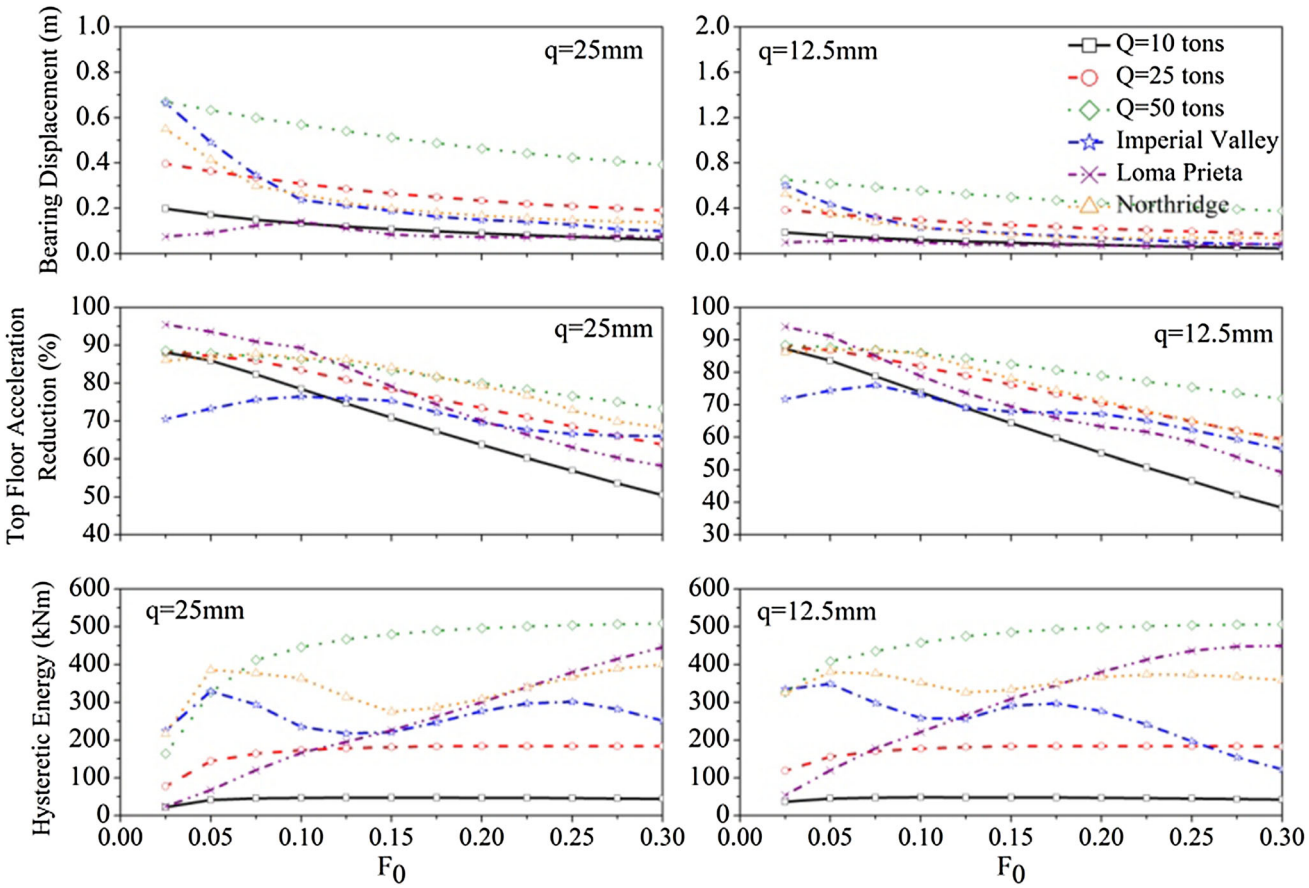

Fig. 12 Effect of yield displacement (q) on the structural responses of a five-storey base-isolated structure ($\xi_b = 4\%$)

References

1. IS 4991: Criteria for Blast Resistant Design of Structures for Explosions Above Ground. BIS, New Delhi (1968).
2. IS 6922: Criteria for Safety and Design of Structures Subject to Underground Blast. BIS, New Delhi (1973)
3. Department of Defense: Structures to Resist the Effects of Accidental Explosions. UFC 3-340-02, Washington (2008)
4. FEMA 428: Primer to Design Safe School Projects in Case of Terrorist Attacks. Federal Emergency Management Agency, Washington (2003)
5. NATO: Manual of NATO Safety Principles for the Storage of NATO Ammunition and Explosives. AC/258-D/258, Bonn (1993)
6. Dowding, C.H.: Blast Vibration Monitoring and Control, vol. 297. Prentice-Hall, Englewood Cliffs (1985)
7. Wu, C.; Lu, Y.; Hao, H.; Lim, W.K.; Zhou, Y.; Seah, C.C.: Characterisation of underground blast-induced ground motions from large-scale field tests. Shock Waves **13**(3), 237–252 (2003)
8. Wu, C.; Hao, H.: Numerical study of characteristics of underground blast induced surface ground motion and their effect on above-ground structures. Part I. Ground motion characteristics. Soil Dyn. Earthq. Eng. **25**(1), 27–38 (2005)
9. Carvalho, E.M.L.; Battista, R.C.: Blast-induced vibrations in urban residential buildings. Proc. Inst. Civ. Eng. Struct. Build. **156**(3), 243–253 (2003)
10. Kumar, R.; Choudhury, D.; Bhargava, K.: Prediction of blast-induced vibration parameters for soil sites. Int. J. Geomech. **14**(3), 04014007 (2013)
11. Kumar, R.; Choudhury, D.; Bhargava, K.: Determination of blast-induced ground vibration equations for rocks using mechanical and geological properties. J. Rock Mech. Geotech. Eng. **8**(3), 341–349 (2016)
12. Tian, L.; Li, Z.X.: Dynamic response analysis of a building structure subjected to ground shock from a tunnel explosion. Int. J. Impact Eng. **35**(10), 1164–1178 (2008)
13. Miyamoto, H.K.; Taylor, D.: Structural control of dynamic blast loading using passive energy dissipaters. In: SEAOC 1999 Convention, pp. 299–317 (1999)
14. Mondal, P.D.; Ghosh, A.D.; Chakraborty, S.: Performance of NZ systems in the mitigation of underground blast induced vibration of structures. J. Vib. Control **20**(13), 2019–2031 (2013)
15. Kang, B.S.; Kang, G.J.; Moon, B.Y.: Hole and lead plug effect on fiber reinforced elastomeric isolator for seismic isolation. J. Mater. Process. Technol. **140**(1), 592–597 (2003)
16. Skinner, R.I.; Tyler, R.G.; Heine, A.J.; Robinson, W.H.: Hysteretic dampers for the protection of structures from earthquakes. Bull. N. Z. Nat. Soc. Earthq. Eng. **13**(1), 22–36 (1980)
17. Moon, B.Y.; Kang, G.J.; Kang, B.S.; Kelly, J.M.: Design and manufacturing of fiber reinforced elastomeric isolator for seismic isolation. J. Mater. Process. Technol. **130**, 145–150 (2002)
18. Constantinou, M.C.; Tadjbakhsh, I.G.: Hysteretic dampers in base isolation: random approach. J. Struct. Eng. **111**(4), 705–721 (1985)
19. Wen, Y.K.: Method of random vibration of hysteretic systems. J. Eng. Mech. **102**(2), 249–263 (1976)

20. Kelly, J.M.; Leitmann, G.; Soldatos, A.G.: Robust control of base-isolated structures under earthquake excitation. J. Optim. Theory Appl. **53**(2), 159–180 (1987)
21. Ramallo, J.C.; Johnson, E.A.; Spencer Jr., B.F.: "Smart" base isolation systems. J. Eng. Mech. **128**(10), 1088–1099 (2002)
22. Ghodke, S.; Jangid, R.S.: Equivalent linear elastic-viscous model of shape memory alloy for isolated structures. Adv. Eng. Softw. **99**, 1–8 (2016)
23. Jangid, R.S.: Optimum lead-rubber isolation bearings for near-fault motions. Eng. Struct. **29**, 2503–2513 (2007)
24. Mohammed, I.; Ikhouane, F.; Rodellar, J.: The hysteresis Bouc–Wen model, a survey. Arch. Comput. Methods Eng. **16**(2), 161–188 (2009)
25. Marano, G.C.; Greco, R.: Efficiency of base isolation systems in structural seismic protection and energetic assessment. Earthq. Eng. Struct. Dyn. **32**(10), 1505–1531 (2003)
26. Uang, C.M.; Bertero, V.V.: Evaluation of seismic energy in structures. Earthq. Eng. Struct. Dyn. **19**(1), 77–90 (1990)
27. Mohamed, A.M.; Mohamed, A.E.E.A.: Quarry blasts assessment and their environmental impacts on the nearby oil pipelines, southeast of Helwan City, Egypt. NRIAG J. Astron. Geophys. **2**(1), 102–115 (2013)
28. Zhang, R.; Phillips, B.M.: Performance and protection of base-isolated structures under blast loading. J. Eng. Mech. **142**(1), 04015063 (2015)
29. Iervolino, I.; Maddaloni, G.; Cosenza, E.: A note on selection of time histories for seismic analysis of bridges in Eurocode 8. J. Earthq. Eng. **13**, 1125–1152 (2009)